ROTORCRAFT SIMULATION MODELLING AND VALIDATION FOR CONTROL DESIGN AND LOAD PREDICTION

Binoy Manimala, Daniel Walker, Gareth Padfield
Department of Engineering, University of Liverpool, Liverpool, UK, L69 3GH

Abstract

This paper describes the development and validation of a high fidelity simulation model of the Bell-412 in the FLIGHTLAB environment for handling qualities and flight control investigations. The base-line rotor model features a rigid, articulated blade-element formulation with flap and lag degrees of freedom. The spring strengths and locations are chosen to match the first flap and lag frequency of the soft-in-plane, hingeless Bell-412 rotor hub. The other key features of the base–line model are the inclusion of lag damper dynamics and a finite state dynamic inflow model. The base-line model gives good agreement for on-axis responses compared with flight test data over the speed range 15-120kt. However, prediction of-off axis responses are less satisfactory. Several model enhancement options available in FLIGHTLAB were introduced to obtain an improved off-axis response. It is shown that the pitch/roll off-axis responses in transient manoeuvres can be improved significantly by including the wake geometry distortion effect in the Peters-He finite state dynamic inflow model.

List of Symbols

C_{eq}	Non-dimensional lag damper coefficient
C_ζ	Lag damping [ft-lbf-s/rad]
d	Lag damper spindle arm [ft]
e_β	Flap hinge offset ratio
e_ζ	Lag hinge offset ratio
I_β	Flap moment of inertia with respect to the flap hinge [slug - ft^2]
I_ζ	Lag moment of inertia with respect to the lag hinge [slug - ft^2]
K_β	Flap hinge spring stiffness [slug – ft^2 / s^2]
K_ζ	Lag hinge spring stiffness [slug – ft^2 / s^2]
$K_{\zeta,f}$	Stiffness provided by the flexi-beam at the yoke of a hingeless rotor [slug – ft^2 / s^2]
K_{eq}	Non-dimensional stiffness
$m(r)$	Blade mass distribution [slug/ft]
M_ζ	Damper moment about the lag hinge [slug - ft]
M_β	First mass moment with respect to the flap hinge [slug - ft]
M_ζ	First mass moment with respect to the lag hinge [slug - ft]
r	Blade element radial location (non-dimensional)
R	Rotor radius [ft]
x	Lag damper displacement [ft]

Paper presented at the 31st European Rotorcraft Forum, 13-15 September 2005, Florence, Italy.

Greek Notation

ψ	Blade azimuth angle [rad]
ζ	Lag angle [rad]
λ_β	First flap frequency ratio
λ_ζ	First lag frequency ratio
Ω	Main rotor rotational speed [rad/s]
ω	Frequency [rad/s]

Introduction

The HELI-ACT project (Helicopter Active Control Technology) being conducted at the University of Liverpool aims to develop advanced control system concepts for helicopters using modern multivariable control techniques. The project consists of a combined theoretical and experimental investigation using state of the art modelling and control tools, exploiting fuselage and rotor-system state feedback. The main aims of the project are to develop a better understanding of the issues relating to helicopter modelling, identification and control of the rotor system and to develop new controls concepts for mutual satisfaction of handling qualities, flight envelope protection and load alleviation. The project involves collaboration with National Research Council Canada (NRC). The project utilises the six-axis motion flight simulator at the University of Liverpool (Ref 1) and NRC's Bell-412 Advanced System Research Aircraft (ASRA) (Ref 2). Use of the fully instrumented ASRA with rotor blade measurements will enable the investigation of some of the deficiencies in existing mathematical models. Better control systems, designed more quickly and with less trial-and-error and flight test development will be achievable if the complexity of the helicopter's dynamics are accurately modelled and taken into account. Hence a high fidelity simulation model of the ASRA (Bell-412 configuration) has been developed in the comprehensive real-time simulation programme FLIGHTLAB (Ref 3). This paper describes the development and validation of that model.

An accurate representation of the dynamics of the vehicle requires, amongst other things, an accurate set of input data comprising the vehicle aerodynamic, structural and configuration details. A large amount of the modelling effort consisted of data collection, mainly from the public domain (published papers and technical reports) and from measurements carried out at NRC Canada. In addition to this, estimates based on engineering knowledge were made when data were not available, so that the simulation predictions produced best fit with the flight test data. These aspects are also described in the paper.

The baseline FLIGHTLAB simulation model of the Bell 412 (designated F-B412) features a rigid, articulated, blade- element rotor formulation with flap and lag degrees of freedom. The spring strengths and locations were chosen to match the first flap and lag frequency of the soft-in-plane hingeless Bell-412 hub (Refs 4 and 5). Another key feature of the baseline model is the inclusion of lag dynamics. The inflow model used is the enhanced Peters–He finite state dynamic inflow model (Ref 6). As will be shown, the baseline model produced very good on-axis responses in comparison to the NRC supplied flight test data over a broad speed range (15-120kt). However, off axis responses were mostly unsatisfactory. Several model enhancement options available in FLIGHTLAB were then introduced to obtain improved off-axis response. The enhancement included modelling of the rotor inflow dynamics in manoeuvres with wake distortion and rotor wake interference on other surfaces, such as the fuselage and horizontal tail. It has been found that the roll/pitch off-axis responses in transient manoeuvres can be improved by including the wake geometry distortion effect in the Peters-He finite state dynamic inflow model.

Description of the model

Bell-412 rotor Hub design

The Bell 412 hub is a hingeless design where the blades are attached to the hub through flexible titanium yokes, known as flexures or flexi-beams, (Ref. 4). The flexures are designed to give an equivalent flap hinge offset that affords good control response but minimises gust responses and oscillatory hub moments transmitted to the fuselage. The blade lag and pitch change motion takes place on one conical/spherical bearing that also retains the blade and transmits centrifugal forces to the yoke. It is a soft in-plane rotor system with the first in-plane mode frequency turned below the 1/rev rotor frequency. Blade lag damping is provided by two identical elastomeric pads, which are housed in bridges that attach to the upper and lower sides of the yoke.

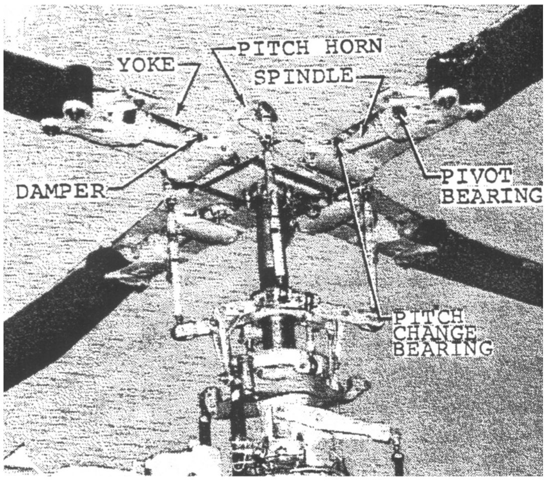

Figure 1: Bell –412 hub (Ref. 4)

Rotor frequencies

The frequencies for the significant rotor modes, reproduced from Ref. 4, are summarised in table 1 below.

Mode	Frequency ratio
1st in-plane	0.6-0.7
2nd in-plane	3.13
1st out-of-plane	1.03
2nd out-of-plane	2.59
3rd out-of-plane	4.47
1st torsion	5.15

Table 1: Rotor frequency ratios for the Bell-412 (Ref 4)

The boundary conditions are cantilevered for the out-of-plane motion and pinned for the in-plane motion; the control stiffness is represented as a spring/damper at the torsional boundary condition

Modelling of the Bell-412 hub and blade retention

A fully coupled elastic model representing the flap, lag and torsional motions is the most accurate way of modelling a hingeless rotor. However, in order to create an elastic blade model it is necessary to have the flap, lag and torsional stiffness and mass distributions, and knowledge of the flexural axis of the blade along its span. In the absence of information on the blade structural properties, a rigid blade model with an equivalent offset hinge and a spring was deemed to be the most appropriate approximation for the elastic deformation of a moderately stiff hingeless rotor blade. Ref. [7] discusses the different ways of modelling all types of blade flap retention systems.

The Bell 412 is relatively 'soft' in the out-of –plane flap motion (frequency ratio of 1.03) and hence an offset hinge and spring analogue model is considered a valid approximation. For the FLIGHTLAB modelling of the 412, the hub is modelled by using equivalent hinge offsets and springs for the flap and the lag motions so that the first frequency ratios are matched.

Selection of flap hinge parameters

Following values for the flap hinge offset ratio, non-dimensionalised with respect to rotor radius, was obtained from Ref [8].

$$e_\beta = 0.046$$

The above value is based on the assumption that the flap hinge and pitch bearing are treated as coincident at the location of the pitch bearing.

Given the above information, the spring constant for the flap hinge can be obtained by matching the frequency ratio of the first mode in the flap degree of freedom.

The expression for the first flap frequency ratio (λ_β) for the flap motion is given by (Ref 7):

$$\lambda_\beta^2 - 1 = \frac{e_\beta}{I_\beta} M_\beta + \frac{K_\beta}{I_\beta \Omega^2} \qquad (1)$$

Where,

$I_\beta = \int_{e_\beta}^{1} m(r - e_\beta)^2 dr$, the flap moment of inertia with respect to the flap hinge, $M_\beta = \int_{e_\beta}^{1} m(r - e_\beta) dr$ is the first mass moment with respect to the flap hinge offset and Ω is the rotor speed.

The spring stiffness that gives the desired first flap frequency ratio is obtained substituting the known values into Equation [1]. It may be noted that the spring stiffness is a negative value here. The yoke, which is flexible in flap, provide a virtual flap hinge inboard of the pitch bearing.

Equivalent lag hinge stiffness: This section describes how the lag hinge stiffness and damping values were obtained for the F-B412. As mentioned before, the blade lag and pitch change motion take place on a conical/spherical bearing that also retains the blade (Ref. 4). According to Ref [8], this bearing is located at 9.3% of the rotor radius from the hub-centre giving a lag hinge offset ratio of: -

$$e_\zeta = 0.093.$$

The expression for the first lag frequency ratio (λ_ξ) for the lag motion is given by:

$$\lambda_\zeta^2 = \frac{e_\zeta}{I_\zeta} M_\zeta + \frac{K_\zeta}{I_\zeta \Omega^2} \qquad (2)$$

The spring stiffness (K_ζ) is obtained by matching the first lag frequency ratio.

Linear Lag damper model

As mentioned above, the blade lag damping for the Bell 412 is provided by two identical elastomeric dampers. The modelling of elastomeric lag dampers is an area meriting its own research due to the complexity of the changes in material properties with operating conditions (Ref 8). The properties of the elastomeric materials depend on strain amplitude and temperature. In addition to strain amplitude dependence, elastomeric materials also exhibit frequency dependence. The frequency of the first lag mode depends on the stiffness of the damper, which in turn depends strongly on the instantaneous strain amplitude in the elastomer. Ref [8] describes various modelling methods, which effectively capture the material behaviour for a range of strain amplitudes and frequencies, representative of the operating conditions of helicopter elastomeric dampers.

FLIGHTLAB provide a spring-damper component to model a lag damper. The damping coefficient can be either a constant (linear lag damper) or it can be supplied as a non-linear table as a function of frequency. Currently, the constant lag damper option is chosen for the F-B412 model. To obtain the linear lag damper coefficient for the F-B412, the following gross approximation (neglecting the frequency dependence) procedure is adopted from Ref [8].

The damper displacement *x* is directly related to the lag angle through the spindle arm (*d*) by the following equation (assuming ξ to be small)

$$x = d * \zeta$$

Thus, using an equivalent viscous damping approach and considering only lag motion, the damper moment about the lag hinge can be written as follows:

$$M_{\zeta} = (Force) * (moment\ arm)$$
$$= \left(K'x + \frac{K''}{\omega}\dot{x} \right) * d$$
$$= \left(K'd^2\zeta + \frac{K''d^2}{\omega}\dot{\zeta} \right)$$

The term $K''d^2/\omega$ is the equivalent viscous damping from the damper at the frequency ω. The term $K'd^2$ is the stiffness provided by the damper. The total stiffness (K_{ξ}) for the lag motion is:

$$K_{\zeta} = K'd^2 + K_{\zeta f}$$

Here, $K_{\xi f}$ is the stiffness provided by the flexi-beam at the yoke of a hingeless rotor. According to Ref [8], for the Bell–412, the stiffness contribution from the flexi-beam is only 2% of the contribution from the damper. Note that the value of the total stiffness K_{ζ}, which includes the contributions from the elastomeric damper and from the flexi-beam, is obtained by matching the first lag frequency (see the previous section). The Bell-412 rotor has a lag hinge offset of 9.3%, which reduces the overall influence of the damper on the lag frequency and consequently, failure of a damper has little effect on the rotor stability.

The damping term $K''d^2/\omega$ for the Bell-412 is obtained from Ref [8] where the equivalent non-dimensional stiffness and damping coefficients of two different damper configurations were plotted as a function of lag angle.

The non-dimensional stiffness and damping coefficients are defined as:

$$K_{eq} = \frac{K'd^2}{I_{\zeta}\Omega^2}$$

$$C_{eq} = \frac{K''d^2}{\omega I_{\zeta}\Omega}$$

Using an damping coefficient of 0.075 (from the plot given in Ref [8]), the damping term, $K''d^2/\omega$ is obtained as:

$$\frac{K''d^2}{\omega} = 0.075 * I_{\zeta}\Omega = 1467.6\ \frac{ft - lbf - s}{rad}$$

Since there are two elastomeric dampers per blade for the Bell 412 rotor, the damping value used for the FLIGHTLAB damper component is twice the above value:

$$C_{\zeta} = 2935.1\ \frac{ft - lbf - s}{rad}$$

It is assumed here that the damping coefficient remains constant over all flight conditions, which in practice is a questionable assumption. In forward flight, the combined 1/rev amplitudes and higher frequency perturbations will reduce the damping significantly - known as a dual frequency effect (see Ref [8]).

Blade aerodynamics

For the baseline model, a Quasi-Steady aerodynamic component was used for the airload calculation on the blade elements. The blade aerodynamic segments are defined based on the equal annuli area approach. This means that the segment length becomes finer towards the tip of the blade. The aerodynamic loads are calculated by treating the blade sections as two-dimensional panels. The blade is divided into several segments and each segment is treated as a two-dimensional panel producing aerodynamic loads as non-linear functions of angle of attack, dynamic pressure and Mach number. The 2D aerofoil table should include lift, drag and pitch moment coefficients as functions of angle of attack and Mach number.

Airfoils

According to Ref [4], the Bell 412 blade contains two airfoils – the BHT 674 airfoil for the inner sections and Wortmann FX-080 towards the tip. The BHT 674 airfoil is a Bell proprietary airfoil very close to the

Boeing VR-7 airfoil. The FX-080 airfoil is believed to be a modified version of either the Wortmann FX-71-H-080 or the FX-69-H-080 (8% thick with a slight camber). Due to lack of information on these airfoils, VR7 aerofoil data (Ref 9 and 10) are used as a substitute for the BHT 674 and a 9% thick cambered airfoil (OA309 airfoil) data are used for the tip aerodynamic segments. The airfoil data were represented in table look-up form with lift, drag and pitching moment coefficients tabulated against angle of attack (-180 to 180deg) and Mach number (0-0.9 Mach).

Inflow model

Rotor inflow modelling has been an area of extensive research carried out over the past three decades. Considerable progress has been made in this area, starting from the classical actuator disk theory in which the inflow of air is assumed to be uniform over the rotor disk. More recent developments include dynamic inflow models which account for low-frequency wake effects under transient conditions. Among various rotor wake solutions, the Peters-He finite state dynamic wake model (Ref. 6) and the distorted vortex wake models, such as described in Refs. [11], [12], and [13], represent major advances in practical rotor wake analysis/simulation technology.

The Bell-412 model described in this work makes use of the Peters-He finite state dynamic wake model. This model captures the uniform and first harmonic distribution of the inflow and the transient response of these inflow components in manoeuvring flight. This methodology also models the dynamic response of the inflow to manoeuvring flight and predicts the off-rotor components of inflow for use in interference modelling at the fuselage and tail.

Tail Rotor

FLIGHTLAB's Bailey rotor component is used to model the tail rotor. The Bailey rotor model is based on the analysis described in Ref [14]. In the Bailey model, closed form expressions for rotor thrust and torque are obtained analytically by integrating the airloads over the rotor blade span and averaging them over the azimuth. Only rotor coning is considered and hence there is no provision for blade cyclic pitch inputs. The induced velocity is computed from a uniform inflow model and included in the model. The following assumptions are employed in the derivation of the tail rotor equations:

1) Constant chord and linear twist
2) Linear lift with lift curve slope
3) Incompressible flow
4) No individual blade dynamics, except for the steady state coning.
5) Uniform induced flow over the rotor

Fuselage

There are several modelling options available within FLIGHTLAB for the fuselage aerodynamics, including a panel method and a simple table look-up. For the Bell-412 model, the table look-up option was chosen where the fuselage coefficients are supplied by means of look-up tables as functions of angle of attack and sideslip angle.

Several reports were used to obtain the fuselage aerodynamic characteristics of the Bell-412 aircraft. Ref [15] gives the longitudinal aerodynamic coefficients for several fuselages of Bell helicopters. Unfortunately, the body drag polar trend has been referenced to minimum drag and thus only represents the increment in drag due to angle of attack. This drag increment, which includes hub and landing gear, has been non-dimensionalised by projected frontal area and dynamic pressure. Ref. [16] reports the results from the wind tunnel tests of two full-scale helicopter configurations conducted at the NASA AMES 40 by 80 foot Wind Tunnel facility. For the wind tunnel tests, a full-scale mock up of a lightweight observation helicopter (LOH) served as one test vehicle and a medium weight utility class helicopter (MUH) served as the other. The LOH was a full-scale mock up the Bell HO-4, built with production construction techniques and the MUH was a Bell UH-1 helicopter.

.

Data from Ref. [17] were used for the side force and yaw moment coefficients of the F-B412 fuselage model. This NASA report presents the results of the wind tunnel investigation of three different fuselage models in the presence of a rotor wake. Out of the three fuselage models tested, representing three helicopters widely used by the US army, the second wind tunnel model was a scaled version of the Bell UH-1 helicopter. Forces and moments of the fuselage and the rotor were measured at wind speeds of up to 102 knots through $\pm$180deg sideslip angles.

Horizontal stabiliser

The Bell 412 uses an inverted Clark-Y airfoil for the tail section (Refs.18 and 19) with a Gurney flap fitted on the trailing edge. The stabiliser is attached to a spring loaded tube so that the incidence is determined by the aerodynamic pitching moment and the spring rate of the spring-loaded tube. The exact location of the elevator and its dimensions were obtained from Ref. [19]. For the NRC Bell-412, the left and the right elevator have different incidences. It was determined by the NRC (Ref. 18) that the left elevator has an incidence of 5.6°and the right elevator has an incidence of –2.4°. The spring constant was determined by NRC by applying known moments to the stabiliser and recording the angular displacement.

The lift and drag coefficients of the Clark-Y airfoil are obtained from Ref. [20]. The data given in Ref. [20] were obtained by wind tunnel experiments on a full-scale wing of aspect ratio 4. The experiment covered a large range of angle of attack (–45° to +90°). Higher angle approximations were used to obtain the lift and drag coefficients outside this range. The effect of the Gurney flap was modelled by modifying the aerodynamic data to incorporate the change in pitching moment and lift curve slope. The horizontal stabiliser spring is modelled by the use of a FLIGHTLAB spring-damper component.

Vertical Fin

The location and dimensions of the vertical fin were obtained from Ref. 19. The aerodynamic characteristics of the fin airfoil are not known at this point and hence it was decided to use the UH60 fin aerodynamic data. The UH60 uses a modified NACA 0021 airfoil for its fin section. Ref. 21 gives the lift and drag polar of this airfoil for a range of –90° to 90° angle of side-slip. For the F-B412 implementation, these data are extended for the whole –180 -180deg.

Propulsion

The F-B412 model currently features an ideal, constant-speed, engine model, which instantaneously provides the required torque and power to the main and tail rotor. It is acknowledged that this is a major shortcoming of the current model and work is underway to develop a suitable engine-rotorspeed governor system model based on flight measurements of the response to collective inputs.

Aerodynamic interference

Modelling the aerodynamic interactions is a challenging aspect of rotorcraft simulation. A simple and effective way of interactional modelling is by incorporating look-up tables representing the downwash/up-wash velocities at the respective aerodynamic surfaces, defined by the values of loads on the generating surface. In the absence of empirical/experimental data, the off-rotor induced velocity predicted by FLIGHTLAB's inflow model is used for the calculation of the effect of the main rotor wake on fixed aerodynamic surfaces. From the finite state dynamic wake equations the induced velocity at an arbitrary flow field point can be computed (Ref. 22). The base-line F-B142 model utilizes this finite-state dynamic inference model for the main rotor wake effects. The main rotor wake interference is applied to both the empennage and the fuselage.

Aircraft Moments of Inertia

There were no data available on the mass moment of inertia of the NRC's Bell-412 aircraft. The NRC aircraft is heavily instrumented and hence it is thought that the inertias will be different than the standard Bell-412. For the F-B412 model the inertias were obtained by a trail and error fashion until the simulation model predicted similar value of short term roll, pitch and yaw response as the test data. NRC supplied the aircraft operating weights and CG positions.

Model validation

The baseline F-B412 model was calibrated against flight test data supplied by NRC Canada. The supplied data mainly contained 3-2-1-1 type inputs at low (around 15kts), medium (around 60kts) and high (90-120kt) speeds with the stability augmentation system (SAS) switched off. In addition, there were some trim data. The input data contained pilot stick positions (measured in inches) rather than blade pitch angles. To facilitate a direct flight mechanics comparison, the mechanical control system of the Bell-412 had to be represented in FLIGHTLAB. To enable this, NRC made available measurements of the mechanical gearings between the pilot control position and the blade pitch motion. The actuators were modelled as a first order lag with a 17Hz bandwidth, which is representative of the actuators chosen for the ASRA.

Trim Comparisons

Comparison of the F-B412 trim attitude predictions against the NRC measurements are given in Fig 2.

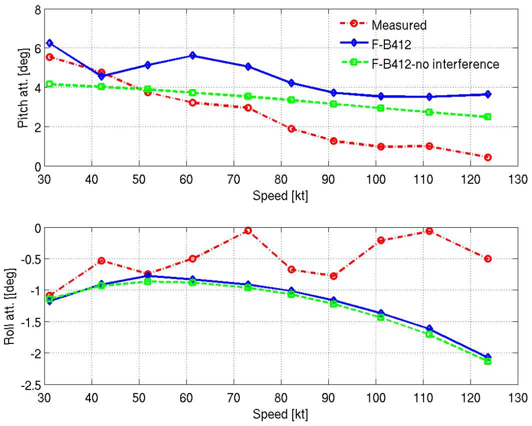

Figure 2: Trim attitudes – predicted and measured

The measured data are compared with predictions for the baseline F-B412 model with and without interference effects of the main rotor wake on the fuselage and the empennage. The pitch attitude predicted using the rotor inference on the horizontal stabiliser and the fuselage shows an improved comparison, particularly at speeds up to 40kt. However, at higher speeds there are large differences between the measured and predicted values. It is considered that the errors may be due to the following reasons:

1) Incorrect fuselage drag for this range of angle of attack.
2) Modelling deficiencies in the spring loaded Bell-412 horizontal stabiliser.
3) Potential for variations in sideslip angle occurring in the trim flight test data, which would lead to variations in roll angle; the simulation tests were flown at zero sideslip.

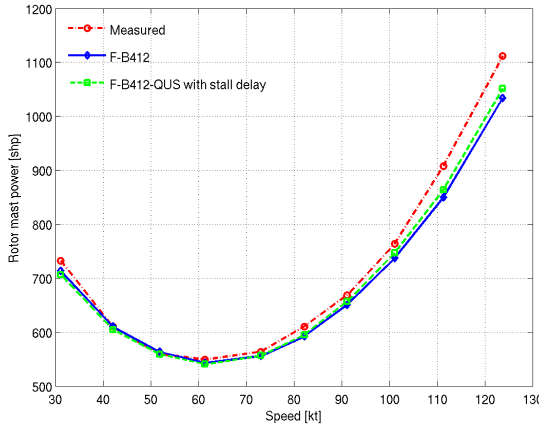

Figure 3: Main rotor mast power – measured and predicted.

Fig 3 shows the main rotor mast power predicted by the F-B412 models and the measured values. There is very good agreement for speeds up to 80kt. This shows that the aerodynamic characteristics of the airfoils used in the F-B412 model are a good representation of the 'real' Bell-412 blades. At higher speeds, when portions of the rotor disc are more heavily loaded, it is generally difficult to predict the power accurately for the following reasons:

1)) Accurate blade aerodynamic data is required at higher Mach numbers. Drag divergence and associated drag rise needs to be accurately represented.

2) Unsteady aerodynamics and stall delay: A unique phenomenon associated with rotorcraft is stall delay resulting from the boundary layer change caused by rotor rotation which adds 3D effects to the blade unsteady aerodynamics. Dynamic stall is also distinguished by a delay in the onset of flow separation to a higher angle of attack than would occur statically.

In FLIGHTLAB it is possible to model unsteady blade aerodynamics and 3D stall delay effects. From Fig 3, it can be seen that the inclusion of the quasi-unsteady blade aerodynamics with stall delay slightly improves the power prediction at higher speeds.

The comparison of power at 120kts shows about 5% error that is not consistent with the pitch angle comparison. So this suggests that the tail plane angle is really to blame for the discrepancy in Fig 2.

Dynamic response

The response of the baseline F-B412 to control inputs is compared against the NRC measurements and the results are shown in Figs 4-8. The roll response at around 60kt and 120kt are shown in Figs 4 and 5. The on-axis responses show good correlation between the flight test data and the base line F-B412 model. The roll to pitch coupling shows reasonably good trend, but the magnitudes differ. The yaw coupling seems to be out of phase with a sharper initial response in flight. This is almost certainly related to the over-simplicity of the engine model.

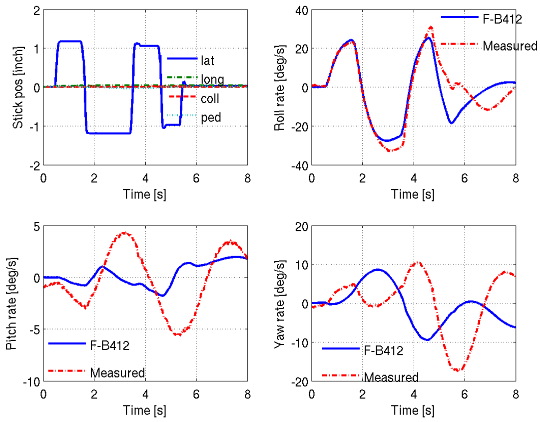

Figure 4: Dynamic Response at 60kt – Roll input.

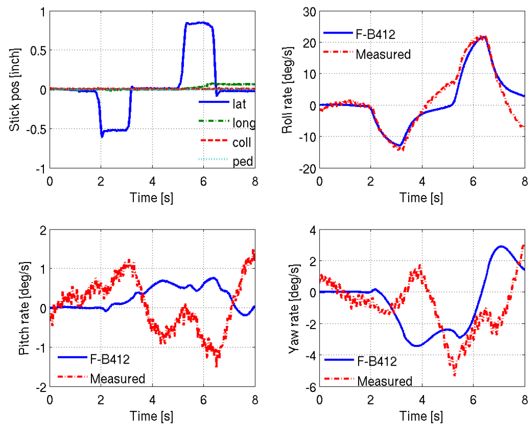

Figure 5: Dynamic Response at 120kt – Roll input

The pitch responses at 60 and 90kt are shown in Figs 6 and 7.

Once again there is a good match for the on-axis response. The prediction of the pitch to roll coupling is again poor, although slightly better than the roll to pitch. There is significantly more yaw response in flight at the lower speed. At the higher speed, the pilot has made inputs in all four controls and the predicted yaw appears to be unstable.

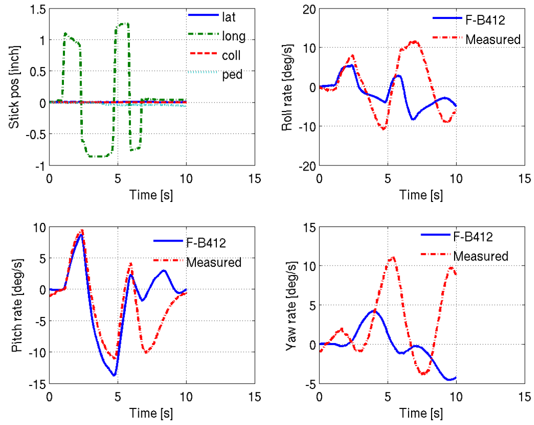

Figure 6: Dynamic Response at 60kt – Pitch input.

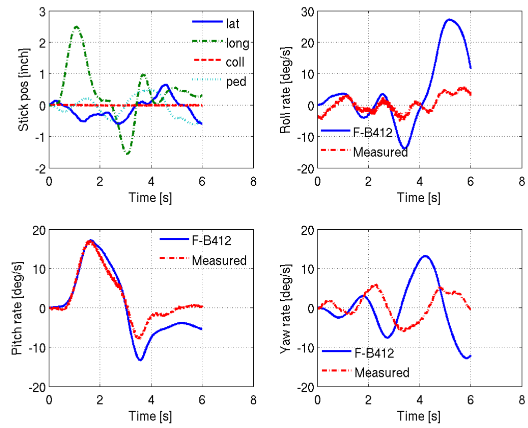

Figure 7: Dynamic Response at 90kt – Pitch input.

The responses of the simulation model and the test aircraft to a pedal input at a flight speed of 60kts are shown in Fig 8. The simulation model predicts the peak of the yaw rate accurately but the yaw damping seems to be slightly different. Also, the measured yaw rate seems to exhibit a slight time delay. The yaw to roll coupling is well predicted by the simulation. The good comparison in the yaw rate in response to pedal reinforces the suspicion that the poor yaw response to pitch is more related to the engine/rotorspeed governor modelling.

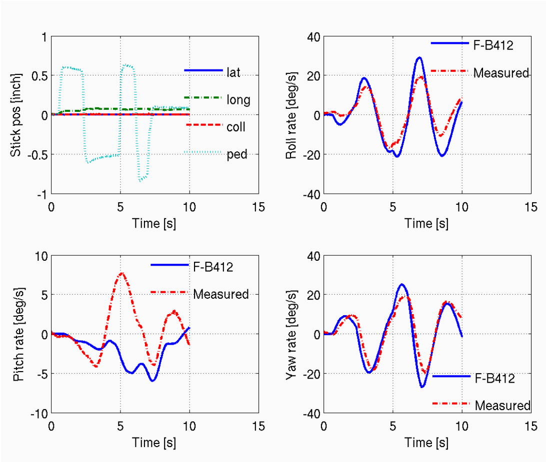

Figure 8: Dynamic Response at 60kt – Yaw input.

Off-axis response

Until fairly recently, most blade-element type helicopter simulation models were unable to predict correct off-axis response (roll response to a pitch input or pitch response to a roll input). These models generally predicted the off-axis angular rates in the wrong direction. The problem has attracted close attention and efforts in resolving it. These investigations have revealed that the discrepancy between the test data and simulation in the off-axis response correlation is mostly related to the rotor aerodynamics at low speed. When the rotor tip-path plane tilts due to the application the cyclic control, the rotor wake distorts in a dynamic fashion resulting in an induced velocity variation over the rotor disk. Various models have been applied to describe the distortion of the rotor wake in transient manoeuvre flight, caused by the applied moments and the rotor passing closer to the blade tip vortices. Comprehensive vortex methods are capable of better representations of off-axis response, since they inherently include the distortion of the wake due to angular motion of the tip-path plane. For the present, it is difficult to see how such formulations, involving considerable additional complexity, could be incorporated into the type of flight mechanics models required for controller design and handling qualities investigations, certainly those required to run in real-time. In recent years, progress has been made towards correcting the off-axis response in flight mechanics simulation models using empirical corrections. Introducing an aerodynamic phase lag and applying a correction factor to the dynamic inflow are two such methods (Ref. 23).

Ref [24] attempts to resolve the deficiencies in off-axis response and aerodynamic interaction through improvement of the Peters-He finite state dynamic wake model. In this approach, the rotor wake distortion effects are accounted for 'on-line' in the rotorcraft simulation code's finite state dynamic inflow model via influence coefficients calculated off-line using a manoeuvre vortex wake model. The enhanced finite state dynamic wake model considers the transient wake distortion and inherently addresses the source of the off-axis rotor moments, while providing a more computationally efficient approach than a vortex wake model. These enhancements have been integrated into the F-B412 model.

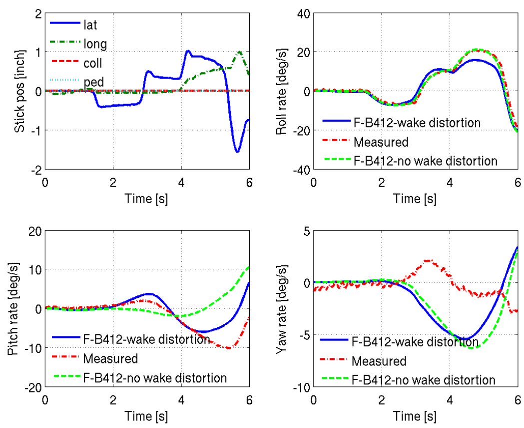

Figure 9: Roll to pitch coupling at 15kt with and without dynamic wake distortion effect.

Fig 9 shows the difference in the off-axis response when wake distortion effect is included in the finite-state dynamic inflow model for a roll input at around 15kt. The solid blue line represents the baseline F-B412 response with the wake distortion 'ON' and the dashed green line gives the response with the wake distortion effect 'OFF'. It can be seen that the model without the wake distortion effect predicts a pitch rate response opposite to the test data. The finite state inflow model that includes the wake geometry distortion effect clearly improves the off-axis response.

Fig 10 shows the off-axis response when wake distortion effect is included for a roll input at around 60kt. Again, considerable improvement is predicted with the wake distortion model.

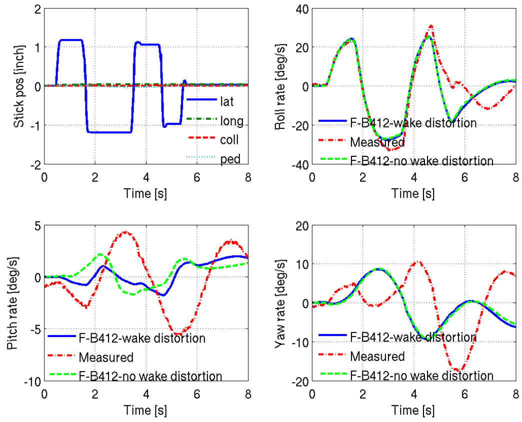

Figure 10: Roll to pitch coupling at 60kt with and without dynamic wake distortion effect.

Conclusions and Future Plans

The paper has described the development and validation of a simulation model of the NRC Bell-412 in the FLIGHTLAB environment. A large part of the modelling effort concentrated on obtaining configuration and aerodynamic data representing the aircraft. Most of the aerodynamic data were obtained from publicly available sources. Measurements were also carried out at NRC Canada to support the modelling activities. In addition to this, certain parameters (such as the vehicle inertias) were estimated so as to make the model predictions match the measured data.

The current base-line model produced excellent on-axis responses in comparison to the NRC supplied flight test data covering a broad speed range. However, off axis responses were less satisfactory. It has been found that the pitch/roll off-axis responses in manoeuvres can be improved by including the wake geometry distortion effect in the Peters-He finite state dynamic inflow model. Inclusion of unsteady aerodynamics appeared to have no significant effect on the flight mechanics. The aerodynamic interference effects made noticeable differences in the trim pitch attitude prediction at low speeds. Outstanding trim deficiencies are believed to centre around the tail plane modelling and degree of sideslip in the flight tests. It is thought that inclusion of an engine model will improve the heave axis and also the off-axis yaw predictions.

One of the aims of the HELI-ACT project is to develop a flight envelope protection and structural load alleviation system (Ref 25). In order to achieve this, it is necessary to have a model capable of predicting the rotor loads (for example, the pitch link load and blade bending). A fully coupled elastic model representing the flap, lag and torsional motions is the most accurate way of modelling a hingeless rotor. However, in order to create an elastic blade model it is necessary to have the span-wise flap, lag and torsional stiffness distributions of the blade. The load prediction capabilities of the 'equivalent' rigid articulated model have not been assessed in detail due to the lack of appropriate flight test data. This is a planned activity for the near future.

Inclusion of engine/drive train dynamics and the creation of an elastic (finite element) blade model are two of the future objectives for the modelling work package within the HELI-ACT project.

Acknowledgment

This research is funded by the U.K. Engineering and Physical Sciences Research Council through Research Grant GR/S42354/01. The authors would like to thank Mr Bill Gubbels of NRC Canada for providing flight test data and measurements.

References

1. Padfield, G.D., White, M.D., "Flight Simulation in Academia; HELIFLIGHT in its first year of operation", Aeronautical Journal of the RAeS, Sept 2003
2. Gubbels, A.W., Carignan, S.J.R.P., "The NRC Bell 412 Advanced System Research Aircraft – A New Facility for Airborne Simulation", Canadian Aeronautics and Space Journal, Vol 46, No. 2, Jun, 2000, p106-115.
3. Du Val, R.W., "A Real-Time Multi-Body Dynamics architecture for Rotorcraft Simulation", Proceedings of the RAeS conference- 'The Challenge of Realistic Rotorcraft Simulation', London, U. K. 7-8 November 2001.
4. Cresap, W. L., and Myers, A. W., "Design and Development of the Model 412 Helicopter", Annual Forum of the American Helicopter Society, Vol. 36, May 1980 .
5. Yen, J. G., Weller, W. H., "Analysis and application of compliant rotor technology," 6th European Rotorcraft and Powered Lift Aircraft Forum, Bristol, England, September 1980.

6. Peters, D. A. and He, Chengjian, "Finite State Induced Flow Models Part II: Three dimensional Rotor Disk", Journal of Aircraft, Vol. 32, No. 2, March-April 1995.

7. Padfield, G. D., "Helicopter Flight Dynamics", Blackwell Science Ltd, 1996.

8. Brackbill, C. R., "Helicopter Rotor Aeroelastic Analysis Using a Refined Elastomeric Damper Model ", PhD Thesis in Aerospace Engineering submitted to the Pennsylvania State University, December 2000.

9. Noonan, K. W., "Aerodynamic Characteristics of Two Rotorcraft Airfoils Designed for Application to Inboard Region of a Main Rotor Blade", NASA TP-3009, July 1990.

10. Dadone, L. U., "US Army Helicopter Design Datcom Volume 1 – Airfoils", NASA-CR-153247, May 1976.

11. Scully, M. P., "A Method of Computing Helicopter Vortex Wake Distortion," ASRL TR138-1, June 1967.

12. Bhagwat, M. J. and Leishman, J. G. "Rotor Aerodynamics During Manoeuvring Flight Using Time Accurate Free-Vortex Wake," Proceedings of the 57th Annual Forum of the AHS, Washington D.C., May, 2001.

13. Johnson, W., "Wake Model for Helicopter in High Speed Flight", NASA CR- CR-1177507, Nov. 1988

14. Bailey, F. J, Jr. "A simplified theoretical method of determining the characteristics of a lifting rotor in forward flight", NACA Report 716, 1941.

15. Harris, F. D., Kocurek, J. D., McLarty, T. T. and Trept, T. J., "Helicopter Performance methodology at Bell Helicopter Textron, American Helicopter Society, 35th Annual Forum, 1979.

16. Biggers, J. C., McCloud, J. L., and Patterakis, P., "Wind-Tunnel Tests of Two Full-Scale Helicopter Fuselages", NASA TN D-1548, 1962.

17. Wilson, J. C. and Mineck, R. E., "Wind-Tunnel Investigation of Helicopter-Rotor Wake Effects on Three Helicopter Fuselage Models", NASA TM X-3185, 1975.

18. Gubbels, A. W. and Auriti, L., "Bell 412 Calibrations", Private communications with NRC Canada. October 2004.

19. Anonymous, "Bell412 EP Product Data". October 2002.

20. Knight, M., Montgomery and Wenzinger, C. J., "Wind-tunnel tests on a series of wing models through a large angle of attack range. Part I : force tests", NACA Report 317 , 1930.

21. Howlett, J. J., "UH-60A Black Hawk Engineering Simulation Program: Volume 1 - Mathematical Model", NASA-CR-166309

22. He, Chengjian, "Finite State Dynamic Wake Interference Modeling for Rotorcraft Simulation", American Helicopter Society 53rd Annual Forum, Virginia Beach, VA, April 29-May 1, 1997.

23. Schulein, G. J., Tichler, M. B., Mansur, M. H. and Rosen A., "Validation of cross-coupling modeling improvements for UH-60 flight mechanics simulations", Journal of the American Helicopter Society, Vol.47, No. 3, July 2002, p 209-213.

24. He, Chengjian, Lee, C. S. and Chen, Weibin, "Rotorcraft simulation model enhancement to support design, testing and operational analysis", Journal of the American Helicopter Society, Vol.45, No. 4, October 2000, p 284-292.

25. Voskuijl, M., Walker, D. J., Manimala B. and Kureemun, R., "First Step Towards the Design of an Active Pitch Link Load Reduction System Using Novel Control Techniques," 31st European Rotorcraft Forum, Florence, Italy, 2005.